Secondary Structure and Location of a Magainin Analogue in Synthetic Phospholipid Bilayers†

Donald J. Hirsh,‡ Janet Hammer,§ W. Lee Maloy,|| Jack Blazyk,*,§ and Jacob Schaefer*,‡

Department of Chemistry, Washington University, St. Louis, Missouri 63130, Department of Chemistry, College of Osteopathic Medicine, Ohio University, Athens, Ohio 45701, and Magainin Pharmaceuticals, Inc., Plymouth Meeting, Pennsylvania 19462

Received June 20, 1996⊗

ABSTRACT: Magainins are cationic, membrane-active peptides which show broad-spectrum antimicrobial activity. We have investigated the secondary structure and location of an analogue of magainin 2 in synthetic phospholipid bilayers using a combination of Fourier transform infrared (FTIR) spectroscopy and solid-state nuclear magnetic resonance (NMR) spectroscopy. Ala_{19}-magainin 2 amide exhibits both α-helix and β-sheet secondary structures in lipid bilayers containing either dipalmitoylphosphatidylglycerol (DPPG) or a 1:1 molar mixture of DPPG and dipalmitoylphosphatidylcholine (DPPC). The combination of FTIR and solid-state NMR results suggests that there are two populations of peptide. The secondary structure of one population is α-helix while that of the other population is β-sheet. We demonstrate that the solid-state NMR technique, rotational-echo double resonance (REDOR), can be used to measure both intra- and intermolecular dipole−dipole interactions in membrane-bound peptides. Our REDOR experiments indicate that α-helical Ala_{19}-magainin 2 amide is bound near the phospholipid head groups.

Magainins are peptides isolated from the skin of the African clawed frog, *Xenopus laevis*, which show broad spectrum antimicrobial activity (Giovannini et al., 1987; Zasloff, 1987). Analogues of magainins are attractive candidates for therapeutic antibiotics and anticancer agents because they inhibit the growth of bacteria, fungi, protozoa (Chen et al., 1988; Zasloff, 1987), and cancer cells (Baker et al., 1993) at concentrations which do not lyse erythrocytes or peripheral blood lymphocytes.

The existing experimental evidence indicates that the antimicrobial activity of the magainins depends on their ability to make the target cells permeable to ions (Baker et al., 1993; Bessalle et al., 1990; Wade et al., 1990). Several observations suggest that this increase in ion transport is *not* mediated by direct or indirect interactions between the magainins and existing ion transport proteins in the cell. First, the magainins are effective against a wide variety of pathogens (Baker et al., 1993; Zasloff, 1987). Second, the potency of magainins and their analogues is correlated with their ability to form cationic amphipathic α-helices (Chen et al., 1988), not on the presence of any specific amino acid sequence. Third, magainins synthesized with all D-amino acids have been found to be as potent as those synthesized with all L-amino acids (Baker et al., 1993; Bessalle et al., 1990; Wade et al., 1990). Fourth, the magainins facilitate the passage of ions through protein-free phospholipid bilayers (Matsuzaki et al., 1989; Wade et al., 1990).

One mechanism proposed for magainin-induced ion transport is that the peptides form ion channels composed of transmembrane α-helices (Cruciani et al., 1992). Recent reports in the literature support this mechanism. In the ion channel model proposed by Matsuzaki et al. (1995), ion channel formation is driven by the concentration gradient of magainin that exists between the outside and the inside of the phospholipid bilayer. This model proposes that the magainin peptides initially bind to the outer surface of lipid vesicles as α-helices, insert transiently as oligomeric ion channels across the bilayer, and then dissociate to the inner surface. In the ion channel model proposed by Ludtke et al. (1994), magainin peptides initially bind as α-helices parallel to the bilayer surface at low peptide to phospholipid ratios and then insert as transmembrane α-helices at higher peptide-to-phospholipid ratios.

Both of these models presume that the peptides which participate in ion transport are α-helical. Indeed, there is some spectroscopic evidence to support this view. Solid-state NMR[1] experiments with oriented lipid bilayers indicate that magainins are completely α-helical (Bechinger et al., 1993). However, circular dichroism (Duclohier et al., 1989; Matsuzaki et al., 1991), FTIR (Jackson et al., 1992), and Raman spectroscopy measurements (Williams et al., 1990) indicate that both α-helix and β-sheet or turn structures are present in membrane-bound magainins.

Ala_{19}-magainin 2 amide (hereafter referred to as Ala_{19}-magainin) is an analogue of magainin 2 amide in which alanine replaces glutamic acid at position 19 (Cuervo et al., 1990). The amino acid sequence of Ala_{19}-magainin is shown in Figure 1. We present here the results of FTIR and solid-state NMR experiments performed with this magainin analogue in multilamellar vesicles (MLVs) of dipalmi-

† This work was supported by National Institutes of Health Grant GM-51554 (J.S.). D.J.H was supported by a National Research Service Award, No. #5F32AI09135, from the National Institute of Allergy and Infectious Disease.

‡ Washington University, St. Louis.

§ Ohio University.

|| Magainin Pharmaceuticals, Inc.

⊗ Abstract published in *Advance ACS Abstracts,* September 1, 1996.

[1] Abbreviations: Ala_{19}-magainin, Ala_{19}-magainin 2 amide; ATR-FTIR, attenuated total reflectance-Fourier transform infrared; CPMAS, cross-polarization magic angle spinning; DPPC, dipalmitoylphosphatidylcholine; DPPG, dipalmitoylphosphatidylglycerol; FTIR, Fourier transform infrared; MIC, minimum inhibitory concentration; MLV, multilamellar lipid vesicle; NMR, nuclear magnetic resonance; REDOR, rotational-echo double resonance; ssb, spinning side-band; T_m, phase transition temperature

S0006-2960(96)01468-7 CCC: $12.00

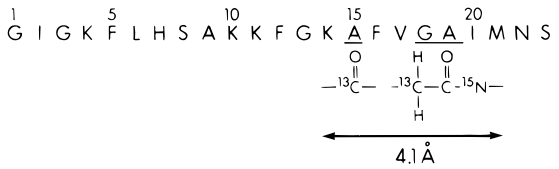

FIGURE 1: Primary structure of Ala_{19}-magainin and the location of ^{13}C and ^{15}N isotopic labels in the labeled peptide. The isotopic labels are identified in the text as [1-^{13}C]Ala_{15} (carbonyl label), [2-^{13}C]-Gly_{18} (methylene label), and [^{15}N]Ala_{19}. In an idealized α-helix, the distance between [1-^{13}C]Ala_{15} and [^{15}N]Ala_{19} is approximately 4.1 Å.

toylphosphatidylglycerol (DPPG) alone and an equimolar mixture of dipalmitoylphosphatidylcholine (DPPC) and DPPG. Our motivations were three-fold: (1) to determine whether magainins do in fact assume secondary structures other than α-helix when bound to lipid bilayers; (2) to localize these secondary structures within the peptide; and (3) to determine the location of the peptide with respect to the lipid bilayer.

MATERIALS AND METHODS

Peptide Synthesis. Unlabeled Ala_{19}-magainin was synthesized using Fmoc chemistry on an Advanced ChemTech model 90 peptide synthesizer. ([1-^{13}C]Ala_{15},[2-^{13}C]Gly_{18},-[^{15}N]Ala_{19})-magainin was synthesized using tBoc chemistry on an Applied Biosystems model 431A peptide synthesizer. The crude peptides were purified by reverse-phase HPLC. Purity was checked by reverse-phase HPLC, capillary electrophoresis and electrospray mass spectrometry (2405.5 and 2408.9 amu for the unlabeled and labeled peptides, respectively). DPPC and DPPG were used as supplied from Avanti Polar Lipids, Inc.

Antimicrobial Assays. Antimicrobial susceptibility testing against *Staphylococcus aureus* (ATCC 29213), *Escherichia coli* (ATCC 25922), and *Pseudomonas aeruginosa* (ATCC 27853) was performed using a modification of the National Committee for Clinical Laboratory Standards microdilution broth assay. Mueller-Hinton broth (BBL) was used for diluting the peptide stock solution and for diluting the bacterial inoculum. The inoculum was prepared from midlogarithmic phase cultures at an approximate concentration of 1×10^6 CFU/mL. Microtiter plate wells received aliquots of 100 μL each of the inoculum and peptide dilution. The final concentration of peptide solution ranged from 0.25 to 256 μg/mL in 2-fold dilutions. The final concentration of bacteria in the wells was $1-5 \times 10^5$ CFU/mL. Peptides were tested in duplicate. In addition to the test peptide, three standard peptides and a nontreated growth control were included to validate the assay. The microtiter plates were incubated overnight at 37 °C. MIC is defined as the lowest concentration of peptide that completely inhibits growth of the organism.

FTIR Sample Preparation. Unlabeled Ala_{19}-magainin was used for all FTIR experiments. Mixtures of lipid (4.56 μmol) and peptide (0.4 μmol) were codissolved in 2:1 $CHCl_3/CH_3OH$ to produce a molar lipid-to-peptide ratio of 11.4:1. For ATR measurements, mixtures were spread on a ZnSe crystal, evaporated to dryness, and hydrated as indicated. For transmission experiments, solvent was removed by evaporation, followed by evacuation under high vacuum, and then mixtures were suspended in D_2O buffer (20 mM PIPES, 1 mM EGTA, pD 7.0), incubated at 55 °C for 12 h, and isolated by centrifugation.

FTIR Spectroscopy. Samples were analyzed in a thermoelectrically controlled cell with CaF_2 windows and a 25 μm Teflon spacer. FTIR spectra were collected using a Mattson Polaris FTIR spectrometer with a HgCdTe detector. A total of 250 interferograms were coadded [except for the attenuated total reflectance (ATR) experiments to measure the rate of H→D exchange, where 16 interferograms were coadded] and Fourier-transformed with triangular apodization to generate absorbance spectra with 2 cm^{-1} resolution and data points encoded every 1 cm^{-1}, with a signal-to-noise ratio of better than 500. Lipid phase changes were monitored by the temperature dependence of the frequency of the symmetric methylene C−H stretching band, which was calculated as described previously (Blazyk & Rana, 1987). All other spectral calculations were performed using GRAMS/386 (Galactic Industries, Inc.). Fourier deconvolution (Griffiths et al., 1986) was performed with a gamma of 5.5 and smoothing of 85%. Second-derivative spectra were calculated with a second-order polynomial and a 27-point window (Savitsky et al., 1964). Curve fitting was performed using the Levenberg−Marquardt method with a Gaussian band shape (Marquardt, 1963).

Measurement of Peptide Binding to Lipids. Lipid−peptide mixtures hydrated with 0.5 mL of D_2O buffer and incubated as described above were filtered using a 1.5 mL microfiltration tube with a 0.45 μm nylon membrane. All of the lipid in the sample was trapped on the filter. Any unbound peptide passed through the filter along with excess solvent. The amount of peptide in the filtrate was measured using the micro BCA assay (Pierce) with bovine serum albumin as standard. Also, the relative amount of lipid to peptide in the sample was estimated by comparing the areas of the carbonyl band from the lipid ester linkages to the amide I′ band from the peptide. Phosphorus content in lipid stock solutions was measured by the method of Chen et al. (1956).

NMR Sample Preparation. Ala_{19}-magainin, with or without isotopic labels, was incorporated into MLVs containing an equimolar mixture of DPPC and DPPG in the following manner. The lyophilized peptide was added to a chloroform solution of the phospholipids in a round bottom flask. The solvent was removed by rotary evaporation and storage under vacuum overnight. The solid mixture of phospholipids and peptide was resuspended in an equal weight of buffer (20 mM PIPES, 1 mM EDTA, pH 7.0) at 60 °C. The resulting suspension was then subjected to five cycles of freezing, warming to $T > T_m$, and mixing with a vortex mixer. Freezing was performed on dry ice. For all NMR samples, the molar ratio of phospholipids to Ala_{19}-magainin was 11.4:1. Samples were packed into a 7-mm high-performance zirconia rotor and fitted with plastic (Kel-F) end caps and spacers. The samples contained approximately 10 μmol of isotopically labeled Ala_{19}-magainin.

NMR Spectroscopy. Experiments were run at 4.7 or 7.0 T using wide-bore Oxford magnets (Oxford, England). The pulse generator and acquisition system for the 4.7-T system are from Tecmag (Houston). The console for the 7.0-T magnet is from Chemagnetics (Fort Collins, CO). Data acquisition was performed with four-channel, transmission line probes which permitted ^{31}P, ^{13}C, and ^{15}N detection or dephasing and ^{1}H dipolar decoupling. The magic-angle stators were obtained from Chemagnetics.

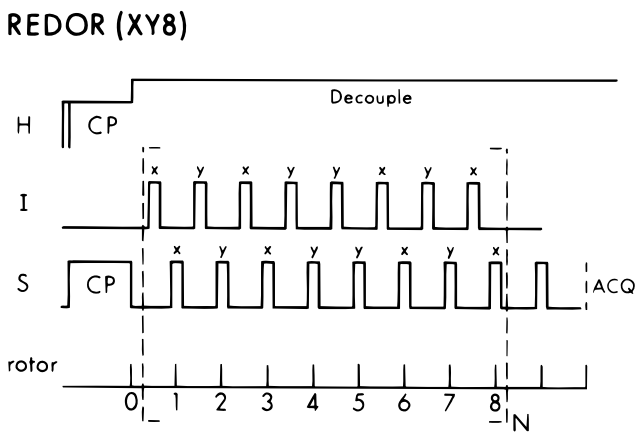

FIGURE 2: REDOR pulse sequence with dephasing π pulses on the I channel and refocusing π pulses on the S channel. The pulses are applied using an XY8 phase cycling scheme to eliminate the effects of offsets and pulse imperfections. Signal acquisition begins two rotor cycles after the completion of a full 8N rotor cycles of dephasing.

NMR spectra were acquired at a controlled magic-angle spinning (MAS) speed of 5000 Hz. Matched spin-locked cross polarization (CP) was performed at 38 kHz with a contact time of 2 ms. ^{13}C spectra were referenced to an external standard, the signal from the ^{13}C label of [4-^{13}C, 4-^{15}N]Asn set to 175.1 ppm. This external standard is in turn referenced to tetramethylsilane (TMS) at 0.0 ppm. Spectra were obtained with a recycle delay of 2 s and ^{1}H decoupling field strength of either 85 or 100 kHz. The decoupling field strengths used with multilamellar dispersions in the gel state and frozen state were 85 kHz; those used with the lyophilized samples were 100 kHz. Spectra were processed with 20 Hz line broadening.

Rotational-echo double-resonance (REDOR) was used to measure the heteronuclear dipolar coupling (D_{IS}) between isolated pairs of labeled nuclei in solids spinning at the magic angle. The basic experiment consists of preparation of transverse S-spin magnetization by cross-polarization (CP) of the S spins from the abundant proton reservoir, followed by a period of I−S dipolar evolution that reintroduces the weak heteronuclear dipolar coupling removed by MAS and then S-spin signal detection (see Figure 2). (In these experiments the S spins were ^{13}C and the I spins were either ^{15}N or ^{31}P.) The dipolar evolution period contains two sets of rotor-synchronized pulse trains; one set of I-spin π pulses in the middle of each rotor cycle and one set of S-spin π pulses at the end of each rotor cycle. (Placing the dephasing pulses at half-rotor period intervals maximizes the dephasing during the dipolar evolution time.) REDOR requires that two spectra be collected, one with pulses on the I channel to produce the spectrum S and one without to produce the spectrum S_o. In a powder, the ratio of the difference between the two spectra ($\Delta S = S_o - S$) and S_o can be directly related to D_{IS} (Pan et al., 1990). Given D_{IS}, the internuclear distance (r_{IS}) can be easily calculated: $r_{IS} = [(\gamma_I\gamma_S h)/4\pi^2 D_{IS}]^{1/3}$, where γ_I and γ_S are the gyromagnetic ratios of the I and S spins, respectively, h is Planck's constant, and the dipolar coupling, D_{IS}, is in Hz.

Natural abundance ^{13}C is present in the peptide and can contribute to both S_o and ΔS if there is chemical shift overlap with the signal arising from the ^{13}C-labeled nucleus. If the $\Delta S/S_o$ value measured in the presence of the isotopic label and the $\Delta S/S_o$ due to natural abundance nuclei are small, approximate corrections (McDowell et al., 1996) to measured $\Delta S/S_o$ values can be made as follows: $(\Delta S/S_o)_{obs} - (\Delta S/S_o)_{na} = (\Delta S/S_o)_{label}$, where $(\Delta S/S_o)_{obs}$ is the value measured experimentally in the presence of the isotopic label, $(\Delta S/S_o)_{na}$ is the value calculated or measured experimentally in the absence of label, and $(\Delta S/S_o)_{label}$ is the dephasing arising only from the labeled nucleus.

Table 1: Antimicrobial Activity

organism	MIC value (μg/mL) magainin 2 amide	MIC value (μg/mL) Ala$_{19}$-magainin 2 amide
Staphylococcus aureus	>256	64
Escherichia coli	64	4
Pseudomonas aeruginosa	128	16

RESULTS

Antimicrobial Activity. As shown in Table 1, Ala$_{19}$-magainin shows the same broad-spectrum antimicrobial behavior that is observed for magainin 2, one of the two peptides originally isolated from the skin of *Xenopus laevis*. In addition, it shows significantly greater activity. Therefore, Ala$_{19}$-magainin is a good model for this class of cationic antimicrobial peptides.

Peptide Binding. At a ratio of 11.4 mol/mol lipid to peptide, Ala$_{19}$-magainin was completely bound (>95%) in lipid dispersions containing either DPPG alone or an equimolar mixture of DPPC and DPPG. With DPPC as the sole lipid component, peptide binding was negligible (<5%). Thus, it is clear that electrostatic attraction between the cationic peptides and negatively charged head groups of DPPG plays a critical role in the initiation of binding.

Solid-State NMR—Secondary Structure. Solid-state NMR experiments were used to monitor the secondary structure of residues 15−19 in ([1-^{13}C]Ala$_{15}$,[2-^{13}C]Gly$_{18}$,[^{15}N]Ala$_{19}$)-magainin 2 amide (see Figure 1). Figure 3 shows ^{13}C spectra for this isotopically labeled Ala$_{19}$-magainin in MLVs containing DPPC and DPPG under three sets of conditions. From solid-state ^{13}C NMR spectra of pure ([1-^{13}C]Ala$_{15}$,[2-^{13}C]-Gly$_{18}$,[^{15}N]Ala$_{19}$)-magainin 2 amide and of DPPC/DPPG dispersions without added peptide, we know that the peaks at approximately 45 and 177 ppm in the gel-state spectrum arise from [2-^{13}C]Gly$_{18}$ and [1-^{13}C]Ala$_{15}$, respectively. The rest of the major peaks in the gel-state spectrum can be assigned to natural-abundance ^{13}C in DPPC and DPPG. In the frozen MLVs, peak intensity increases at approximately 172 and 43 ppm, and resonances arising from the phospholipid head group (50−70 ppm) are broadened. Upon lyophilization of the MLVs there is a slight decrease in intensity at 172 and 43 ppm.

MLVs of DPPC/DPPG containing unlabeled Ala$_{19}$-magainin were also prepared and lyophilized. A ^{13}C spectrum of this sample shows signals arising only from natural-abundance ^{13}C. Subtraction of this ^{13}C spectrum from that of an identical sample containing *labeled* Ala$_{19}$-magainin yields a difference spectrum (Figure 4) showing only the signals arising from the ^{13}C labels in the peptide. The difference spectrum clearly shows two resonances for each ^{13}C label: [1-^{13}C]Ala$_{15}$ gives rise to two peaks at 176.8 and 172.4 ppm, and [2-^{13}C]Gly$_{18}$ shows a peak at 45.4 ppm and a shoulder at 43.5 ppm. These secondary chemical shifts and chemical-shift differences, which are consistent with a

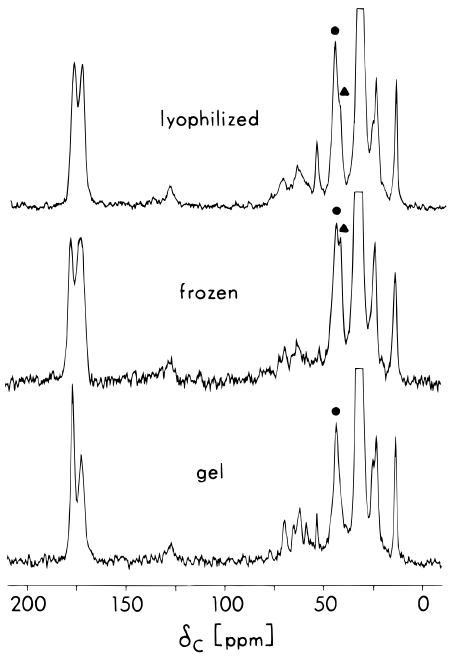

FIGURE 3: 50 MHz ^{13}C CPMAS echo spectra of multilamellar vesicles of DPPC/DPPG:Ala$_{19}$-magainin, 11.4:1, mol/mol. The spectra result from the accumulation of 1636 scans (gel state), 1248 scans (frozen), and 3776 scans (lyophilized). Peaks at 45 ppm (●) and 43 ppm (▲) are marked.

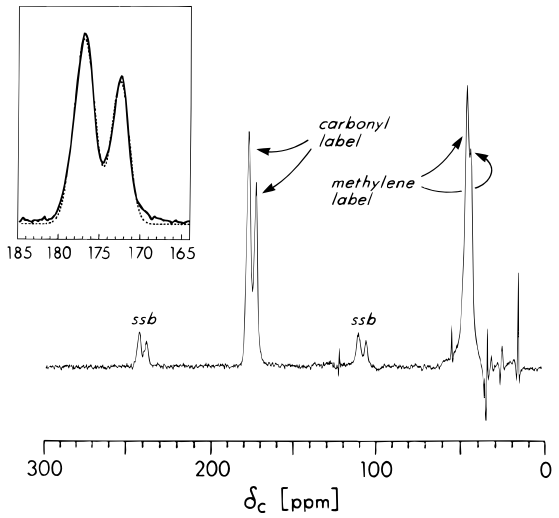

FIGURE 4: 75 MHz ^{13}C CPMAS echo difference spectrum of labeled Ala$_{19}$-magainin in lyophilized multilamellar vesicles of DPPC/DPPG. Prior to subtraction the spectra were scaled by the peak height of the signal arising from the phospholipid methylene carbons at 33 ppm. The peaks at 176.8 and 172.4 ppm and their spinning side bands (ssb) arise from [1-^{13}C]Ala$_{15}$ (carbonyl label). The peak and shoulder at 45.4 and 43.3 ppm, respectively, arise from [2-^{13}C]Gly$_{18}$ (methylene label). The sharp "spikes" are artifacts of the subtraction process (see text) which arise from slightly different lineshapes in the two samples. (Inset) The solid line is the result of summing the peaks at 176.8 and 172.4 ppm with their spinning side bands. The broken line is the best fit by a sum of two Gaussians.

mixture of α-helix and β-sheet conformations (Saito, 1986; Wishart et al., 1994), are summarized in Table 2. When DPPG was the sole lipid component, the ^{13}C difference spectrum for isotopically labeled Ala$_{19}$-magainin was qualitatively the same, i.e., two resonances each for [1-^{13}C]Ala$_{15}$ (176.8 and 172.4 ppm) and [2-^{13}C]Gly$_{18}$ (45.4 and 43.3 ppm) (data not shown). However, the relative intensities within each pair of peaks was not the same.

The ^{13}C difference spectra from DPPC/DPPG/Ala$_{19}$-magainin and DPPG/Ala$_{19}$-magainin were used to quantify the amount of α-helix and β-sheet structure in this region of the peptide. Spinning side bands from the resonances at 173 and 177 ppm, arising from [1-^{13}C]Ala$_{15}$, were added to those at the isotropic chemical-shift positions. The resulting spectra were then simulated as a sum of two Gaussians. The inset to Figure 4 shows the NMR data and the fit for Ala$_{19}$-magainin in MLVs of DPPG/DPPC. Table 3 summarizes the results.

The presence of a directly bonded ^{14}N nucleus can have an influence on the ^{13}C line shape (Frey et al., 1980; Olivieri et al., 1987). In the presence of the ^{14}N quadrupole moment, magic angle spinning may not completely average the carbon−nitrogen dipolar coupling. The strength of the residual dipolar coupling is a strong inverse function of the static magnetic field. We considered the possibility that the line shape of the signal from [1-^{13}C]Ala$_{15}$ was affected not only by the secondary structure of the peptide but also by the residual dipolar coupling between the ^{13}C label and the directly bonded amide ^{14}N. However, spectra collected at 50 and 75 MHz (Figures 3 and 4) for carbon gave the same quantitation of α-helix and β-sheet (Table 3).

If the region of the peptide including the isotopic labels [1-^{13}C]Ala$_{15}$ and [^{15}N]Ala$_{19}$ is α-helical, the distance between ^{13}C and ^{15}N will be 4.1 Å and dipolar coupling will be observable by REDOR. If this region adopts a β-sheet conformation, the dipolar coupling will be too weak to observe. As a further check on the secondary structure of the peptide, ^{13}C observe, ^{15}N dephase REDOR experiments were performed on labeled Ala$_{19}$-magainin in gel state, frozen, and lyophilized MLVs of DPPC and DPPG. Figure 5 shows the ^{13}C observe, ^{15}N dephase REDOR spectra for the lyophilized MLVs. The full ^{13}C spectrum (S_o), obtained 58 rotor cycles after ^{1}H−^{13}C cross-polarization, is shown at the bottom of the figure. The ^{15}N dephased spectrum (S) was also obtained 58 rotor cycles after ^{1}H−^{13}C cross-polarization but with ^{15}N dephasing pulses during the first 56 rotor cycles. The difference between the two spectra, S and S_o, gives the difference spectrum (ΔS) shown at the top of Figure 5. $\Delta S/S_o$ is large at 45 ppm due to the relatively short, fixed distance (2.46 Å) between [2-^{13}C]Gly$_{18}$ (methylene label) and [^{15}N]Ala$_{19}$. As expected for an α-helix, a small difference signal is observed at 176.8 ppm, due to the dipolar interaction between [1-^{13}C]Ala$_{15}$ (carbonyl label) and [^{15}N]Ala$_{19}$. Consistent with the resonance at 172.4 ppm representing [1-^{13}C]Ala$_{15}$ in a β-sheet conformation, no difference signal is observed at this chemical shift.

The dependence of $\Delta S/S_o$ vs. dephasing time for [1-^{13}C]-Ala$_{15}$ at 176.8 ppm is shown in Figure 6 for labeled Ala$_{19}$-magainin in gel state, frozen, and lyophilized MLVs of DPPC/DPPG. The values of $\Delta S/S_o$ ($N_c = 40$) for the three sets of conditions are within experimental error. Measurements from the lyophilized MLVs at three dephasing times were fitted by a polynomial equation which matches the REDOR universal dephasing curve. The fit gives a dipolar coupling of 40 ± 2 Hz, corresponding to a distance of 4.2 ± 0.1 Å between the amide nitrogen of Ala$_{19}$ and the carbonyl carbon of Ala$_{15}$. This distance is consistent with residues 15−19 residing in an α-helix.

Transmission FTIR Spectroscopy—Lipid Fluidity and Secondary Structure. Incorporation of Ala$_{19}$-magainin into MLVs containing either DPPG or DPPC/DPPG causes only

Table 2: ^{13}C Chemical Shift Values for Protein Secondary Structures

	solid[a]			solution[b]			this work[c]		
amino acid	α-helix	β-sheet	Δ	α-helix	β-sheet	Δ	α-helix	β-sheet	Δ
[1-^{13}C]Ala	176.4	171.8	4.6	176.9	172.3	4.6	176.8	172.4	4.4
[2-^{13}C]Gly		43.7		43.8	41.9	1.9	45.4	43.3	2.1

[a] Saito (1986). Data are taken from Table 1. Where more than one value was given for the chemical shift, the median was taken. Chemical shift reference is TMS. [b] Wishart and Sykes (1994). Data are taken from Table VI. Chemical shift values have been adjusted to the chemical shift reference TMS (DSS value minus 2.7 ppm). [c] Chemical shift reference is TMS.

Table 3: Peptide Secondary Structure Content

11.4:1 DPPG:Ala$_{19}$-Magainin 2 Amide

transmission FTIR[a]				ATR-FTIR				NMR		
gel		liquid crystalline		dry		saturated		lyophilized		associated
cm^{-1}	%	cm^{-1}	%	cm^{-1}	%	cm^{-1}	%	cm^{-1}	%	secondary structure
1605	1	1608	1			1604	2			
1634	34	1634	19	1635	6	1636	25	172.4	26	β-sheet
1653	61	1651	75	1657	88	1654	70	176.8	74	α-helix
1678	4	1678	5	1680	6	1678	3			

11.4:1 DPPC/DPPG:Ala$_{19}$-Maginin 2 Amide

transmission FTIR[a]				ATR-FTIR				NMR		
gel		liquid crystalline		dry		saturated		lyophilized		associated
cm^{-1}	%	cm^{-1}	%	cm^{-1}	%	cm^{-1}	%	cm^{-1}	%	secondary structure
1604	1	1605	1			1605	1			
1634	37	1634	21	1636	6	1634	28	172.4	40	β-sheet
1653	57	1651	71	1658	88	1653	66	176.8	60	α-helix
1676	6	1675	7	1681	6	1675	5			

[a] The FTIR data in this table are the averaged values for four samples of 11.4:1 DPPG:Ala$_{19}$-magainin 2 amide and four samples of 11.4:1 DPPC/DPPG:Ala$_{19}$-magainin 2 amide. The largest standard deviations for the areas of the components near 1635 and 1650 cm^{-1} are ±3% and ±5%, respectively.

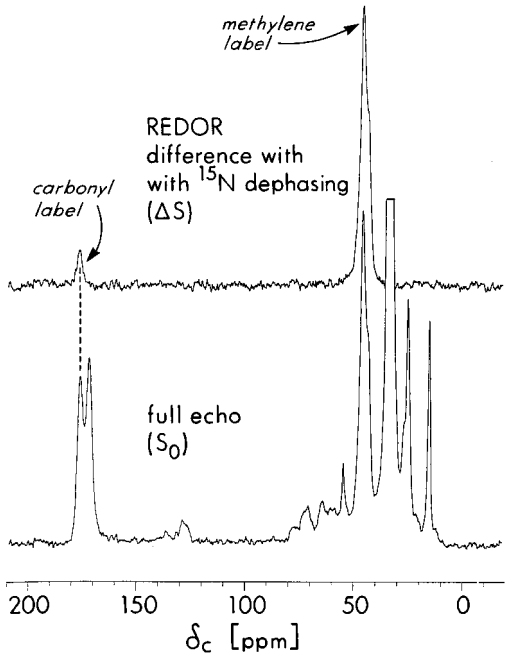

FIGURE 5: ^{13}C observe, ^{15}N dephase REDOR spectrum of Ala$_{19}$-magainin in multilamellar vesicles of DPPC/DPPG. The resonant frequency for carbon is 50 MHz. ΔS is the ^{13}C difference spectrum after 56 rotor cycles of ^{15}N dephasing and a two rotor cycle echo. S_o is the ^{13}C full echo spectrum after 58 rotor cycles. The full echo spectrum results from the accumulation of 80 000 scans.

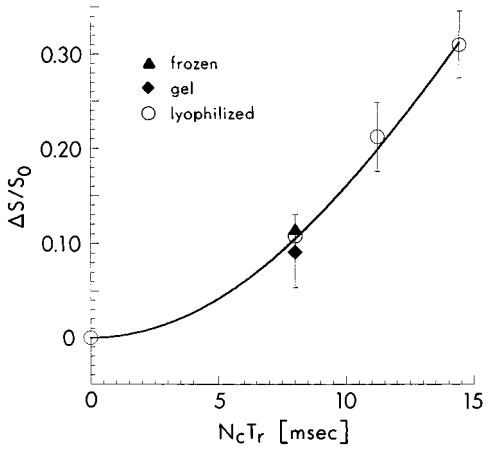

FIGURE 6: S/S_o vs dephasing time (N_cT_r) for Ala$_{19}$-magainin in multilamellar vesicles of DPPC:DPPG. N_c is the number of rotor cycles of dephasing and T_r is the rotor period. $\Delta S/S_o$ was measured at $N_c = 40$ for gel state (◆) and frozen (▲) multilamellar dispersions. $\Delta S/S_o$ was measured at $N_c = 40$, 56, and 72 for the lyophilized vesicles (○), and the line shows the best fit of the theoretical dephasing curve to these data.

a slight reduction in T_m, from 41 to ~37−38 °C, suggesting that the peptide does not significantly disrupt the bilayer structure. MLVs containing Ala$_{19}$-magainin in excess D_2O buffer show no amide II band, indicating the complete exchange of the amide NH groups by deuterium. The conformationally sensitive amide I′ band was analyzed as a function of temperature (Figure 7). When the lipids are in the gel state, the band is centered near 1650 cm^{-1}, with a large shoulder near 1635 cm^{-1}. Above T_m, the magnitude of the shoulder decreases. Fourier deconvolution reveals four components between 1600 and 1700 cm^{-1} (Figure 8). The areas represented by these components are summarized in Table 3. In both lipid systems, the major component is a band centered at ~1651−1653 cm^{-1}, which is attributable

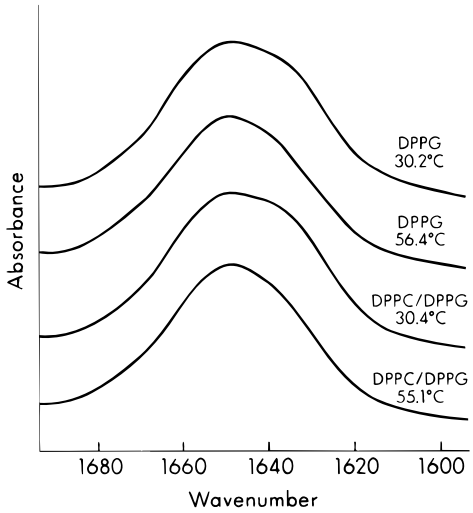

FIGURE 7: Amide I′ band of D_2O dispersions of 11.4:1 phospholipid:Ala_{19}-magainin.

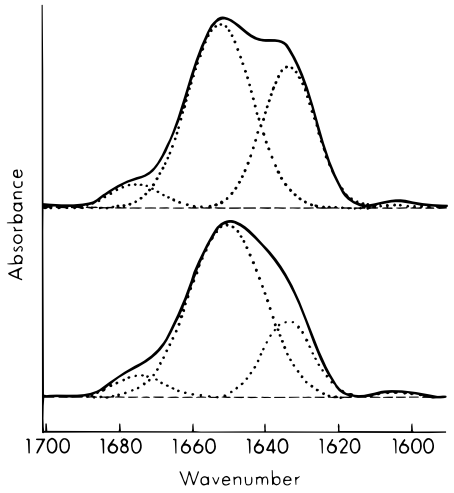

FIGURE 8: Curve fitting of deconvolved amide I′ bands of 11.4:1 DPPC/DPPG:Ala_{19}-magainin at 30.4 °C (top) and 55.1 °C (bottom). The relative areas of the four fitted peaks under each band are listed in Table 3.

to α-helical conformation (Krimm & Bandekar, 1986). Below T_m, this band comprises about 60% of the total area, but increases to 71−75% as the lipids enter the liquid crystal phase. The 1634 cm^{-1} component, which is generally associated with β-sheet structure (Krimm & Bandekar, 1986), accounts for about 35% of the total area in the gel state, and diminishes to about 20% above T_m. The areas of the other two components, near 1675 and 1605 cm^{-1}, constitute less than 8% of the total area in each case. The change between the two band shapes coincides with the lipid phase change (data not shown). The increase in α-helical content appears to be a direct consequence of the increase in lipid fluidity.

ATR-FTIR Spectroscopy. Quantitation of peptide secondary structure by solid-state NMR was done using lyophilized samples. To make a more direct comparison between FTIR and solid-state NMR determinations of secondary structure, ATR-FTIR was used to study lipid/peptide mixtures in varying states of hydration. The effects of hydration on peptide conformation were studied by first examining the amide I′ band of dry lipid−peptide mixtures in which the amide nitrogens are fully proteated. Figure 9 shows the results for 11.4:1 DPPC/DPPG:Ala_{19}-magainin. The amide I band is relatively narrow and centered at 1657 cm^{-1}. The

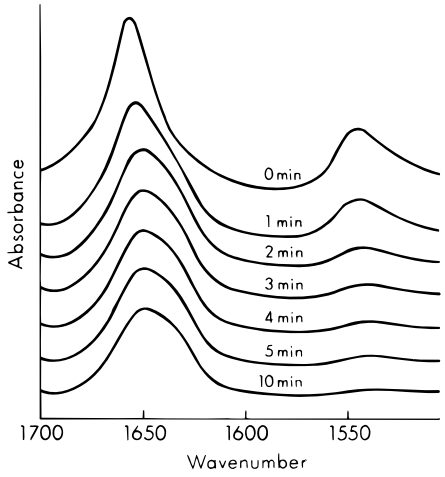

FIGURE 9: ATR-FTIR spectra of 11.4:1 DPPC/DPPG:Ala_{19}-magainin on a ZnSe crystal under anhydrous conditions (top) and exposed to a saturated D_2O atmosphere for variable amounts of time. The temperature was 22 °C.

α-helical content of the peptide in the anhydrous sample is estimated at 88% by curve-fitting analysis (see Table 3). Essentially identical results were obtained for the peptide in DPPG.

To determine the accessibility of the peptide to added solvent, the ATR crystal was sealed at 22 °C in a D_2O atmosphere by enclosing a strip of D_2O-saturated filter paper which did not come into contact with the sample. Spectra were recorded as a function of time to determine changes in the amide I and amide II bands. The data in Figure 9 show that the exchange of amide protons with deuterons occurs within minutes. The area of the amide II band is reduced by more than 60% over the first 2 min and to less than 10% of its original area after 10 min. The band is no longer detectable after 30 min of exposure. This observation means that the peptide has access to the aqueous surroundings and that the amide NH groups are not locked in hydrogen bonds which impede the exchange process. In addition, the shape of the amide I′ band changes dramatically with hydration. The peak maximum shifts downward and a component near 1635 cm^{-1} appears immediately upon hydration, increasing as the amide II band recedes. After 10 min, there is no further change in the amide I′ band. The α-helical content of the D_2O-hydrated peptide, labeled "saturated" in Table 3, is intermediate between the samples below and above T_m, as measured by transmission FTIR. When liquid D_2O is added directly to the sample on the ATR crystal, the amide I′ band in the resulting spectrum is indistinguishable from that observed in the gel state by transmission FTIR.

We believe that the water content of MLVs exposed to D_2O vapor in the ATR-FTIR experiment, labeled "saturated" in Table 3, is comparable to that of the lyophilized samples used in the solid state NMR experiments. As demonstrated in Figure 9, the dry MLVs show rapid changes in peptide secondary structure upon exposure to water vapor. Since the lyophilized NMR sample was packed on the benchtop over the course of an hour, there was ample opportunity for the NMR sample to absorb ambient water vapor from the air.

Solid State NMR—Location of Peptide in the Lipid Bilayer. Magainins can form a highly amphipathic α-helix with a hydrophobic face and a hydrophilic cationic face. Figure

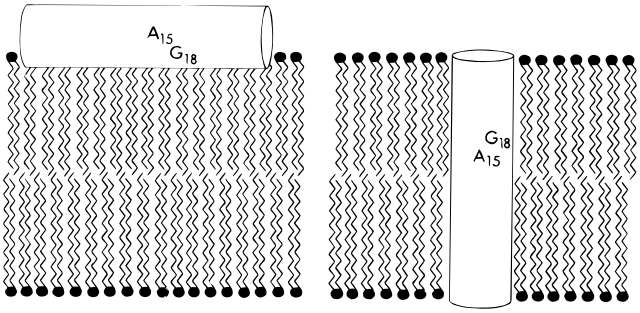

FIGURE 10: Cartoon showing two possible locations for an α-helical peptide (white cylinder) associated with a lipid bilayer: (left) bound near the lipid/water interface and (right) transmembrane.

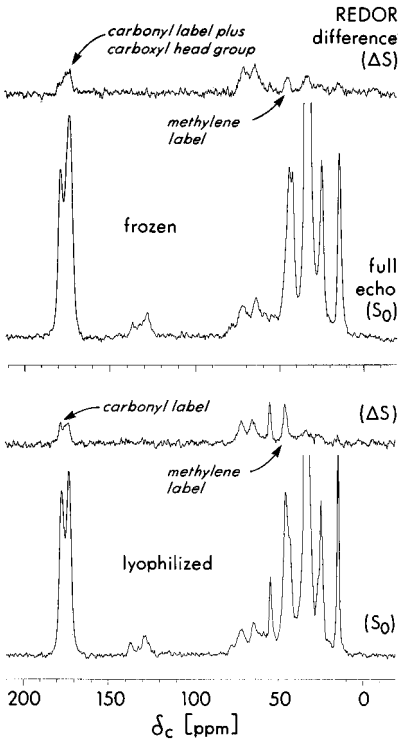

FIGURE 11: ^{13}C observe, ^{31}P dephase REDOR spectrum of Ala_{19}-magainin in frozen and lyophilized multilamellar vesicles of DPPC/DPPG. ΔS is the ^{13}C difference spectrum after 40 rotor cycles of ^{31}P dephasing and a two rotor cycle echo. S_o is the ^{13}C full echo spectrum after 42 rotor cycles. The number of scans accumulated for the full echo spectra were 56 672 (frozen) and 42 704 (lyophilized).

10 illustrates two possible orientations for the peptide in a lipid bilayer. In Figure 10 (left), the peptide lies parallel to the plane of the bilayer at the polar−nonpolar interface. This orientation would place the ^{13}C labels in Ala_{19}-magainin in proximity to the phosphorus atoms of the phospholipid head groups. Alternatively, Figure 10 (right) shows the peptide spanning the bilayer with its helical axis perpendicular to the bilayer plane. This orientation places the ^{13}C labels in Ala_{19}-magainin near the center of the bilayer, much farther away from the phospholipid head groups.

To determine whether Ala_{19}-magainin is associated with the phospholipid head groups, ^{13}C observe, ^{31}P dephase REDOR experiments were performed on frozen and lyophilized MLVs containing labeled Ala_{19}-magainin and DPPC/DPPG. Figure 11 shows the ^{13}C difference (ΔS) and full echo spectra (S_o) for a REDOR experiment with 40 rotor cycles of ^{31}P dephasing for both frozen and lyophilized MLVs. Peaks in the difference spectrum which appear at chemical-shift values corresponding to those of the two ^{13}C labels in the peptide are marked with arrows in Figure 11. The remaining peaks in the difference spectrum arise solely from natural-abundance ^{13}C in the phospholipids which have detectable intra- or intermolecular dipolar couplings to the phospholipid phosphorus.

Table 4: ^{13}C Observe, ^{31}P Dephase REDOR Dephasing in Lyophilized MLVs

	labeled Ala_{19}-magainin 2 amide		unlabeled Ala_{19}-magainin 2 amide	
δ_C	$\Delta S/S_o$	$(\Delta S)_N$[a]	$\Delta S/S_o$	$(\Delta S)_N$[a]
176.8	0.13 ± 0.02	0.10 ± 0.02	0	0
172.4	0.12 ± 0.02	0.11 ± 0.02	0.30 ± 0.03	0.09 ± 0.01
45.4	0.24 ± 0.02	0.19 ± 0.02	0	0

[a] Normalized ΔS. The ΔS peak height was divided by the peak height of the methyl resonance from the phospholipid acyl chains at 14 ppm in S_o.

^{13}C observe, ^{31}P dephase REDOR experiments were also performed on lyophilized MLVs of DPPC/DPPG containing unlabeled Ala_{19}-magainin (spectra not shown). Table 4 lists $\Delta S/S_o$ values for both labeled and unlabeled Ala_{19}-magainin in lyophilized MLVs at the chemical shift positions marked by arrows in Figure 11. Only the 172.4 ppm chemical shift has significant intensity in the full echo spectrum (S_o) of the unlabeled Ala_{19}-magainin sample because it arises from natural-abundance ^{13}C in the fatty acid carbonyl carbons of the phospholipids. As expected, these carbons show significant dephasing ($\Delta S/S_o$) from the phospholipid phosphorus.

Natural-Abundance Correction for β-Strand Peptides. There is significant peak intensity at 172 ppm in S_o and ΔS in the ^{13}C observe, ^{31}P dephase REDOR spectra of unlabeled Ala_{19}-magainin, due to natural abundance ^{13}C in the phospholipids (Table 4). From our investigations of secondary structure, we have assigned [1-^{13}C]Ala_{15} in a β-sheet conformation to approximately the same chemical shift position, i.e., 172.4 ppm. This means that the peaks at 172.4 ppm in the full-echo spectra (S_o) of labeled Ala_{19}-magainin (Figure 11) have contributions from both [1-^{13}C]Ala_{15} in a β-sheet conformation and from natural-abundance ^{13}C in the phospholipids. The difference peak (ΔS) observed with labeled Ala_{19}-magainin at 172.4 ppm in Figure 11 must reflect a contribution from the natural-abundance ^{13}C in the phospholipid, because we observe a difference signal with unlabeled peptide; however, it may or may not reflect a contribution from [1-^{13}C]Ala_{15}.

The question of whether or not [1-^{13}C]Ala_{15} makes a contribution to the difference peak observed at 172.4 ppm in Figure 11 can be addressed by comparing the intensity of the difference peak (ΔS) observed at 172.4 ppm in the sample with labeled Ala_{19}-magainin to that of ΔS with unlabeled Ala_{19}-magainin. To make this comparison, the difference peaks must be normalized. Table 4 shows the difference peaks normalized by the peak height of the phospholipid acyl chain methyl resonance which appears at 14 ppm. The normalized difference peaks at 172.4 ppm are the same, to within the uncertainty in the measurement, for the labeled and unlabeled peptides. Therefore, [1-^{13}C]Ala_{15} attributed to β-sheet does not make a measurable contribution to the difference peak at 172.4 ppm. As for the difference peak observed at 45.4 ppm for labeled Ala_{19}-magainin, we cannot distinguish the contributions of [2-^{13}C]Gly_{18} in α-helical vs

β-sheet conformations because the chemical-shift resolution is insufficient.

DISCUSSION

FTIR and Peptide Secondary Structure. The FTIR results (Table 3) show that membrane-bound Ala_{19}-magainin adopts both α-helical and β-sheet conformations in MLVs containing either DPPG or DPPC/DPPG both above and below T_m. Although an increase in lipid fluidity enhances the α-helical content, β-sheet secondary structure still accounts for ~20% of the overall peptide conformation. Qualitatively similar results were obtained by Jackson et al. (1992) in their FTIR study of magainin 2 amide in DMPG.

Chemical Shifts and Peptide Secondary Structure. The solid-state NMR results show two chemical shifts for each of the ^{13}C labeled residues in Ala_{19}-magainin 2 in lyophilized MLVs containing DPPG (Figure 4), indicating that there are two distinct chemical environments for residues 15 and 18. We propose that the two different chemical environments are the result of differences in secondary structures. The ^{13}C chemical shifts of amino acids have been correlated with secondary structure by both solid-state (de Dios et al., 1993; Saito 1986) and solution-state (Wishart et al., 1994) NMR. For all amino acids, carbonyl carbon and α-carbon ^{13}C chemical shifts move downfield in the transition from a random coil to α-helix. Conversely, there is an upfield shift for the carbonyl carbon and α-carbon in the transition from random coil to β-sheet. As Table 2 indicates, the two chemical shifts observed for [1-^{13}C]Ala_{15} in Ala_{19}-magainin are consistent with those expected for a mixture of α-helix and β-sheet conformations. In the case of [2-^{13}C]Gly_{18}, the upfield shift is consistent with that observed for glycine in a β-sheet conformation in the solid state. The chemical shift difference between the two signals from [2-^{13}C]Gly_{18} in Ala_{19}-magainin is the same as the average chemical shift difference observed for [2-^{13}C]Gly in solution for α-helix and β-sheet conformations.

REDOR and Peptide Secondary Structure. The assignment of the peak at 176.8 ppm to [1-^{13}C]Ala_{15} in an α-helical secondary structure is confirmed by the ^{13}C observe, ^{15}N dephase REDOR experiment (Figures 5 and 6). The $^{13}C-^{15}N$ dipolar coupling between the carbonyl carbon of Ala_{15} and the amide nitrogen of Ala_{19} corresponds to a distance of 4.2 ± 0.1 Å, as expected. The absence of a REDOR difference signal from the [1-^{13}C]Ala_{15} peak at 172.4 ppm indicates that amide nitrogen of Ala_{19} is more than 5 Å away, consistent with this signal arising from [1-^{13}C]Ala_{15} in a β-sheet structure.

Comparison of NMR and FTIR Determinations of Secondary Structure. The FTIR data provide a global view of peptide secondary structure. There is no way of knowing which amino acid residues participate in α-helices and which amino acid residues participate in β-sheets from the FTIR data alone. This is illustrated by panels a and b of Figure 12 for a peptide which shows 66% α-helix and 33% β-sheet conformation, as determined by FTIR. The two secondary structures could arise from two populations of peptide, one population that is completely α-helical and another that is completely β-sheet (panel a) or a single population of peptide in which every molecule contains both types of secondary structure (panel b).

On the other hand, solid state NMR of a specifically labeled peptide provides a local view of peptide secondary structure. While the secondary structure in the vicinity of the isotopic labels can be determined, nothing is known about the global secondary structure. This is illustrated by panels a and c of Figure 12 for a specifically labeled peptide which shows 66% α-helix and 33% β-sheet conformation measured by solid-state NMR. The presence of α-helical or β-sheet structure over a five-residue region (15−19) might reflect the global secondary structure of the peptide (panel a), or it might reflect only the local secondary structure (panel c).

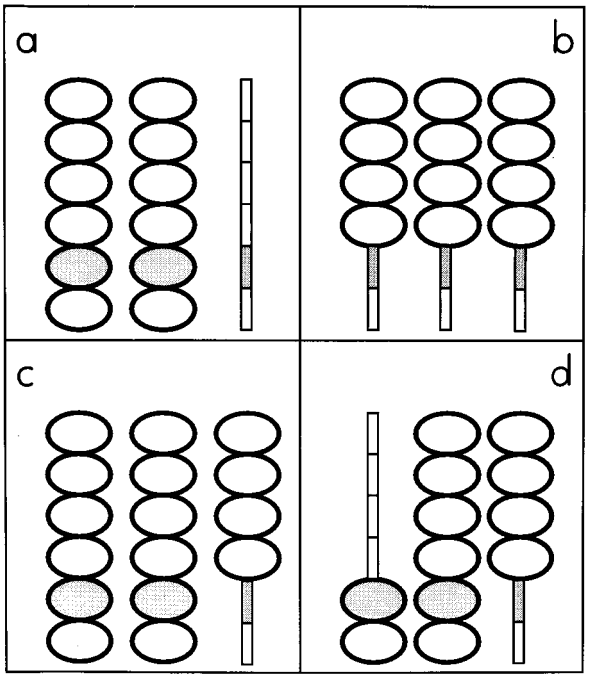

FIGURE 12: Cartoon of possible peptide secondary structures. Ovals represent regions of α-helix: narrow boxes represent regions of β-sheet. The number of amino acid residues in one oval equals the number in one box. Local peptide secondary structure can be monitored in the shaded regions by using isotopic labels.

The secondary structure content of Ala_{19}-magainin determined from ATR-FTIR spectra of D_2O vapor-saturated MLVs and the ^{13}C solid-state NMR spectra of lyophilized MLVs are approximately the same (Table 3). The agreement is best for MLVs with DPPG alone but reasonably good for MLVs containing both DPPG and DPPC, given the uncertainties in the hydration and the curve fitting procedures of the two measurements. Since both FTIR and solid-state NMR experiments measure approximately the same secondary structure content, the simplest model consistent with both measurements is that there are two populations of peptide—one population that is completely α-helical and another that is completely β-sheet, shown in Figure 12a. The FTIR and NMR data cannot rule out a more complicated model, such as that represented in Figure 12d in which there are different populations of peptide molecules, all of which possess a mixture of α-helix and β-sheet structure, but differ in the distribution of these structures within the polypeptide chain. In such a model, however, it would simply be fortuitous for the global and local secondary structure contents to be identical. In the model represented by panel a, this is required. Since Ala_{19}-magainin is only 23 amino acid residues in length, we favor the model shown in Figure 12a because it is less likely that stable segments of both α-helix and β-sheet conformation could coexist within the same peptide molecule.

The changes in peptide secondary structure that are observed by FTIR and solid-state NMR upon dehydration of the MLVs also support the two-state model shown in panel a of Figure 12. In Figure 3, one can see that, in the transition from frozen to lyophilized MLVs, the peaks at 172.4 and 43.5 ppm lose intensity relative to the peaks at 176.8 and 45.4 ppm, respectively. Since the peaks at 172.4 and 43.5 ppm are attributed to [1-^{13}C]Ala_{15} and [2-^{13}C]Gly_{18} in β-sheet, and the peaks at 176.8 and 45.4 ppm are attributed to [1-^{13}C]-Ala_{15} and [2-^{13}C]Gly_{18} in α-helix, lyophilization apparently favors α-helical conformation in the vicinity of these labels. ATR-FTIR results also show that α-helical content increases as hydration decreases (Figure 9). The simplest explanation for this correlation is that the local changes in secondary structure observed by solid-state NMR reflect global changes in peptide conformation.

Solid-State NMR-Location of Peptide in the Lipid Bilayer. ^{31}P dephasing of ^{13}C resonances is observed at 176.8, 172.4, and 45.4 ppm in the REDOR difference spectra of frozen and lyophilized MLVs containing labeled Ala_{19}-magainin (Figure 11 and Table 4). Dephasing ($\Delta S/S_o$) is slightly greater in the lyophilized sample than in the frozen sample, possibly due to differences in the packing between the peptide and the phospholipid head groups in the two samples.

We conclude from the results listed in Table 4 that most of the α-helical Ala_{19}-magainin is in proximity to the phospholipid head groups. If the the α-helical peptides were transmembrane, the $\Delta S/S_o$ values would be more than an order of magnitude smaller than those observed in the ^{13}C-observe, ^{31}P-dephase REDOR experiments (Figure 11). An estimate of the distance between the ^{13}C labels in the peptide and the phosphorus in the phospholipid head group can be made if one assumes that there is a single pair-wise interaction and that all of the α-helical peptides are bound at the polar−nonpolar interface. With this assumption, we calculate a ^{13}C−^{31}P distance of 6.5 Å for [1-^{13}C]Ala_{15} and 5.8 Å for [2-^{13}C]Gly_{18} in the lyophilized MLV. These are reasonable distances for a peptide lying at the membrane surface, given that the peptide ^{13}C labels are near the center of the α-helix and separated from the lipid phosphorus by the side chains of the peptides and the head groups of the lipids.

Previous solid-state NMR studies of magainin 2 amide in oriented phospholipid bilayers (Bechinger et al., 1991, 1993) found α-helical peptides lying parallel to the plane of the bilayer. Our results essentially support those findings except that we also find peptides which are in a β-sheet conformation. Their location and orientation are less certain. However, it does not appear that the β-sheet peptides are closely associated with the phospholipid head groups, at least not in the vicinity of residue 15.

Although our ^{13}C observe, ^{31}P dephase REDOR results indicate that most of the α-helical peptide is associated with the phospholipid head groups, we cannot rule out the possibility that a fraction of the α-helices are transmembrane. We plan to investigate this possibility by incorporating ^{19}F labels into the phospholipid acyl chains and ^{13}C labels into the peptide. We can then use these to look for ^{13}C−^{19}F intermolecular dipolar couplings. We also plan to investigate the oligomerization of the magainin peptides. While the mechanisms of Ludtke et al. (1994) and Matsuzaki et al. (1995) require oligomerization of magainins, this has not been directly observed. In future experiments, REDOR will be used to look for ^{13}C−^{19}F dipolar couplings between peptide molecules.

ACKNOWLEDGMENT

We thank Dr. Dorothy Mac Donald of Magainin Pharmaceuticals for performing the antimicrobial assays.

REFERENCES

Baker, M. A., Maloy, W. L., Zasloff, M., & Jacob, L. S. (1993) *Cancer Res. 53*, 3052−3057.
Bechinger, B., Kim, Y., Chirlian, L. E., Gesell, J., Neumann, J. M., Montal, M., Tomich, J., Zasloff, M., & Opella, S. J. (1991) *J. Biomol. NMR 1*, 167−173.
Bechinger, B., Zasloff, M., & Opella, S. J. (1993) *Protein Sci. 2*, 2077−2084.
Bessalle, R., Kapitkovsky, A., Gorea, A., Shalit, I., & Fridkin, M. (1990) *FEBS Lett. 274*, 151−155.
Blazyk, J., & Rana, F. R. (1987) *Appl. Spectrosc. 41*, 40−44.
Chen, H. C., Brown, J. H., Morell, J. L., & Huang, C. M. (1988) *FEBS Lett. 236*, 462−466.
Cruciani, R. A., Barker, J. L., Durell, S. R., Raghunathan, G., Guy, H. R., Zasloff, M., & Stanley, E. F. (1992) *Eur. J. Pharmacol. 226*, 287−296.
Cuervo, J. H., Rodriguez, B., & Houghten, R. A. (1990) in *Peptides−Chemistry and Biology* (Rivier, J. E., & Marshall, G. R., Eds.) pp 124−126, ESCOM, Leiden.
de Dios, A. C., Pearson, J. G., & Oldfield, E. (1993) *Science 260*, 1491−1496.
Duclohier, H., Molle, G., & Spach, G. (1989) *Biophys. J. 56*, 1017−1021.
Frey, M. H., & Opella, S. J. (1980) *J. Chem. Soc., Chem. Commun. 9*, 474−475.
Giovannini, M. G., Poulter, L., Gibson, B. W., & Williams, D. H. (1987) *Biochem. J. 243*, 113−120.
Griffiths, P. R., & Pariente, G. L. (1986) *Trends Anal. Chem. 5*, 209−215.
Jackson, M., Mantsch, H. H., & Spencer, J. H. (1992) *Biochemistry 31*, 7289−7293.
Ludtke, S. J., He, K., Wu, Y., & Huang, H. W. (1994) *Biochim. Biophys. Acta 1190*, 181−184.
Marquardt, D. W. (1963) *J. Soc. Ind. Appl. Math. 11*, 431−441.
Matsuzaki, K., Harada, M., Handa, T., Funakoshi, S., Fujii, N., Yajima, H., & Miyajima, K. (1989) *Biochim Biophys Acta 981*, 130−134.
Matsuzaki, K., Harada, M., Funakoshi, S., Fujii, N., & Miyajima, K. (1991) *Biochim. Biophys. Acta 1063*, 162−170.
Matsuzaki, K., Murase, O., Fujii, N., & Miyajima, K. (1995) *Biochemistry 34*, 6521−6526.
McDowell, L. M., Klug, C. A., Beusen, D. D., & Schaefer, J. (1996) *Biochemistry 35*, 5395−5403.
Olivieri, A. C., Frydman, L., & Diaz, L. E. (1987) *J. Magn. Reson. 75*, 50−62.
Saito, H. (1986) *Magn. Reson. Chem. 24*, 835−852.
Savitsky, A., & Golay, M. J. E. (1964) *Anal. Chem. 36*, 1627−1639.
Wade, D., Boman, A., Wahlin, B., Drain, C. M., Andreu, D., Boman, H. G., & Merrifield, R. B. (1990) *Proc. Natl. Acad. Sci. U.S.A. 87*, 4761−4765.
Williams, R. W., Starman, R., Taylor, K. M., Gable, K., Beeler, T., Zasloff, M., & Covell, D. (1990) *Biochemistry 29*, 4490−4496.
Wishart, D. S., & Sykes, B. D. (1994) *Methods Enzym. 239*, 363−392.
Zasloff, M. (1987) *Proc. Natl. Acad. Aci. U.S.A. 84*, 5449−5453.

BI961468A